UNIVERSITY OF MINNESOTA
ST. ANTHONY FALLS LABORATORY
Engineering, Environmental and Geophysical Fluid Dynamics

Project Report No. 460

Investigation of a Low-Drag Partially Cavitating Hydrofoil: Water Tunnel Tests

by

Jon Hansberger, Martin Wosnik, Hong Wang and Roger E.A. Arndt

Prepared for
Dr. Eduard Amromin
Mechmath, LLC.

September 2003
Minneapolis, Minnesota

UNIVERSITY OF MINNESOTA
ST. ANTHONY FALLS LABORATORY
Engineering, Environmental and Geophysical Fluid Dynamics

Project Report No. 460

Investigation of a Low-Drag Partially Cavitating Hydrofoil: Water Tunnel Tests

by

Jon Hansberger, Martin Wosnik, Hong Wang and Roger E.A. Arndt

Prepared for
Dr. Eduard Amromin
Mechmath, LLC.

September 2003
Minneapolis, Minnesota

TABLE OF CONTENT

List of Figures

1 Introduction

This project is based on a request made to the Saint Anthony Fall Laboratory by Dr. Eduard Amromin on behalf of Mechmath, Inc. The work was performed under a sub-contract as part of a Phase I SBIR contract with the Defense Advanced Research Projects Agency (DARPA).

Figure 1.1 is the basic contour of OK-2003 hydrofoil. Details of the design are supplied in the progress report from Mechmath and Amromin et al (2003). This hydrofoil is designed to take advantage of the drag reduction that would be possible with a stabilized cavity on the suction side of the profile. In the configuration currently under review the suction side is on the lower surface, hence the design is optimized for negative angles of attack. Figure 1.2 depicts the theoretical pressure distribution at angle of attack -3^{o}. A view of the test hydrofoil is given in Figure 1.3

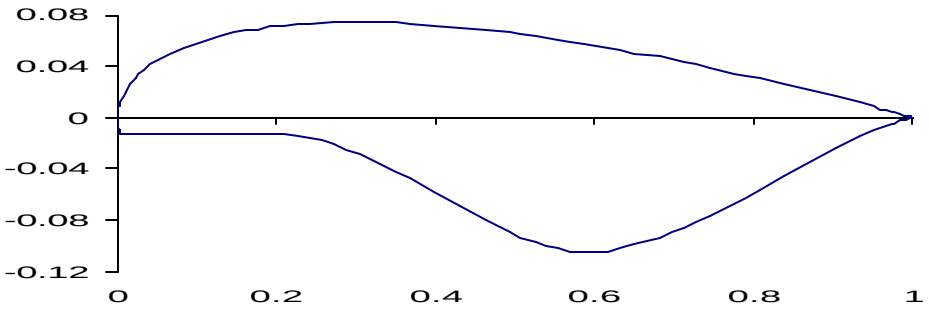

Figure 1.1 Basic contour of the OK-2003 Hydrofoil

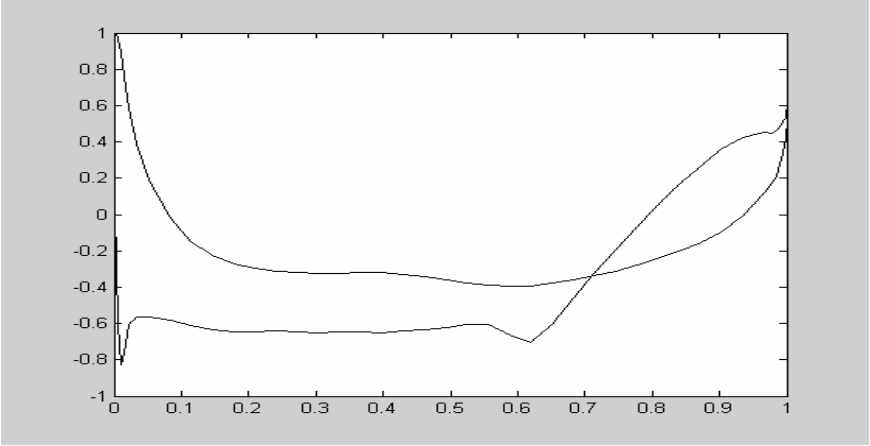

Figure 1.2 Theoretical pressure distribution on the 0K-2003 hydrofoil at an angle of -3 degrees

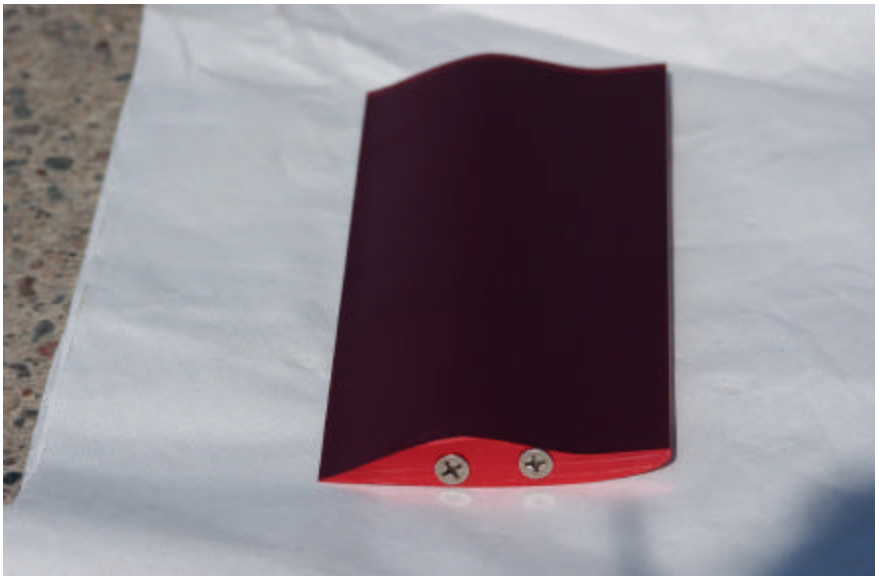

Figure 1.3 View of OK-2003 hydrofoil

2 Procedure

The OK-2003 hydrofoil was mounted and tested in the Saint Anthony Falls Laboratory High Speed Cavitation Tunnel. Lift and drag data, as well as digital still pictures and digital videos were obtained. Lift and drag were measured simultaneously with a force balance. The force balance is calibrated in-situ using weights. There is 20% hysteresis in drag measurement[1], but the lift measurement works very well. Lift and drag were measured at -5, -6, -7 degrees of angle of attack at various cavitation numbers. Time-series data of lift and drag are also obtained for further spectrum analysis.

The force balance measures the normal and longitudinal forces relative to the chord line of the hydrofoil, denoted as L_m and D_m. In order to measure lift and drag relative to the flow direction, the following coordinate transformation is used:

$$L = L_m \cos a - D_m \sin a$$
$$D = L_m \sin a + D_m \cos a$$

Where α is the angle of attack.

Digital still pictures are taken using a Nikon D1H digital SLR camera with the following settings: bulb, f6.3, ISO1250. The flow is illuminated by two stroboscopes triggered by an external power source. Pictures were taken at -5 degrees of angle of attack with various cavitation numbers. A

[1] This is due to mechanical hysteresis and will be corrected in Phase II by using a newly designed lift balance.

Canon GL2 digital camcorder is used to record digital videos. The digital camcorder was positioned normal to the water tunnel back window. A ruler is put in front of the back window to measure the cavity length directly. All the videos herein are made at 30 fps. Three series of videos for -6°@8m/s, -6°@10m/s, and -7°@9m/s were recorded respectively. Video data were sent to Mechmath in CD Rom format.

3 Data analysis

3.1 Angle Of Attack For Zero Lift

The data in Figure 3.1 illustrate that that -3° is very close to the angle of zero lift. Figure 3.1 is the plot of lift vs. velocity at angle of attack 1° (-3° + 4°) and -7° (-3° - 4°) respectively. It shows that these data are symmetric with respect to the x-axis and that zero lift would be obtained at -3°. Actually, the data oscillated from negative to positive values at -3°. Thus this technique was used to verify that the angle of zero lift was -3°.

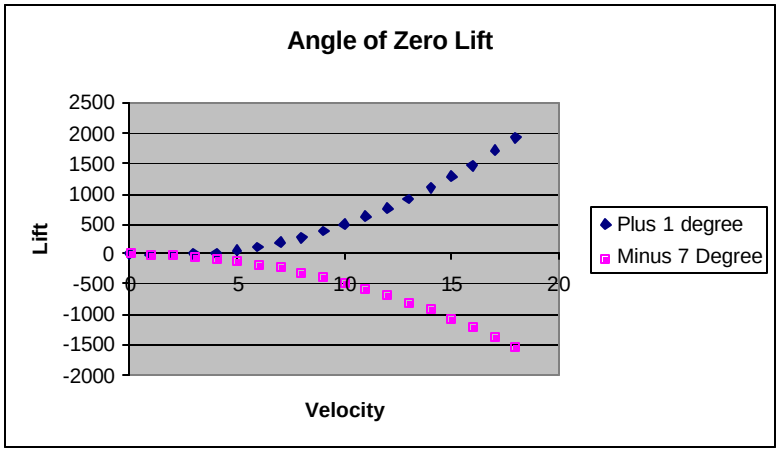

Figure 3.1 Angle of zero lift

3.2 Lift

Figure 3.2 is the plot of lift coefficient vs. sigma. The lift coefficient is defined as:

$$C_l = \frac{Lift}{1/2\,r U^2 ch}$$

Where:

C_l------Lift coefficient
Lift---- Lift on the hydrofoil
?------- Density of water
U------ Velocity of upstream
c------- Cord length(0.081m)
h------- Height of the hydrofoil (0.19m)

Several ways were tried to collapse the data well. As shown in Figure 3.2 a plot of lift coefficient vs. sigma provides the best collapse of the data.

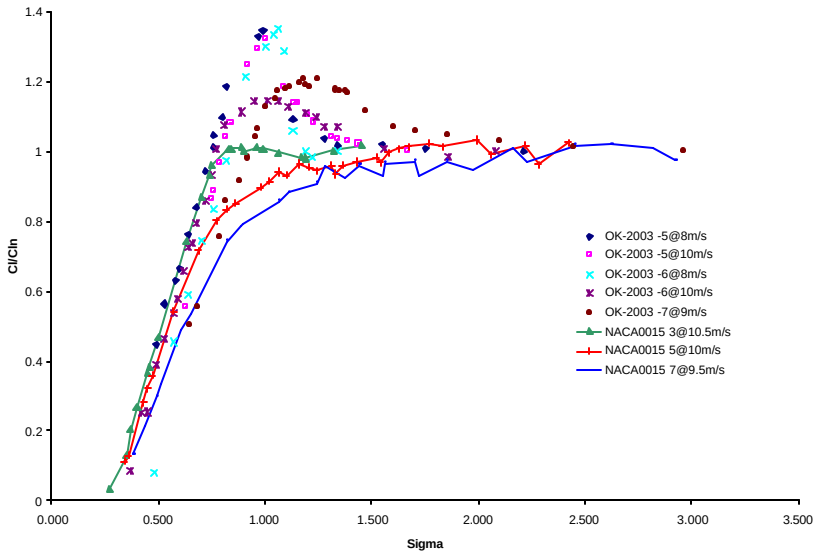

Figure 3.2 Lift coefficient

Note that the maximum negative lift coefficient occurs at around sigma = 1.0 rather than for the non-cavitating condition as is the case for the NACA 0015 profile from which this hydrofoil is derived. Because the maximum lift is a little higher than the upper limit of the lift balance, the peak for -5@12m/s is not as significant as the other data. Improvements to the force balance will be made during Phase II.

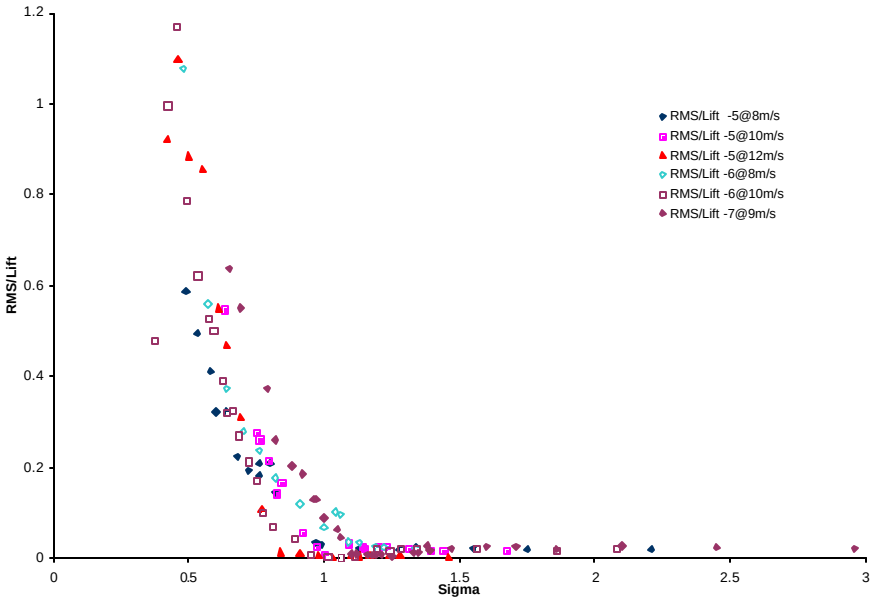

Figure 3.3 RMS Lift vs. Sigma

Figure 3.3 is the plot of RMS Lift normalized to the average value of lift vs. sigma. As sigma is lowered below the maximum lift value, the intensity of lift oscillations increases markedly. When the cavitation number decreases, the cavitation changes from partial cavitation to super-cavitation. The maximum normalized RMS Lift is 1.17 at -6@10m/s with cavitation number 0.45. This indicates that there are very strong oscillations in lift with magnitudes well above the average value.

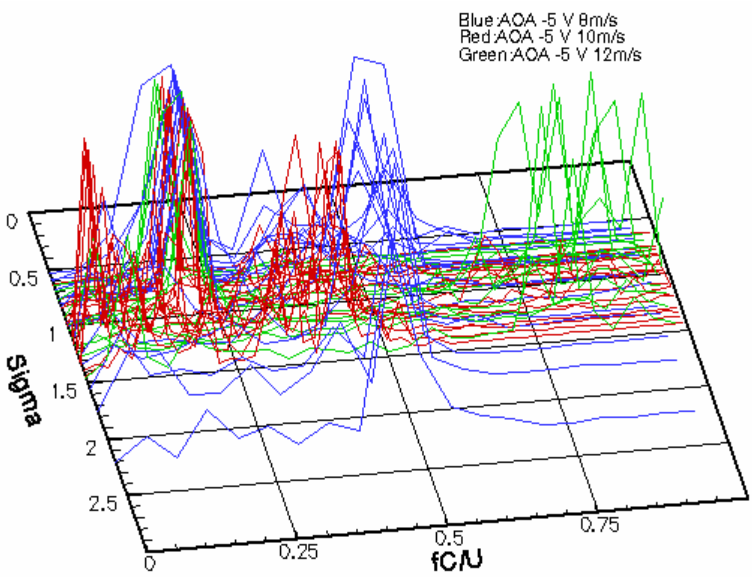

Figure 3.4 Lift spectrum for angle of attack -5°

Spectral lift data are shown in Figure 3.4, obtained at an angle of attack -5º. Since the sample size was small, the resolution of the spectrum plot is not very high. However, it is significant that there are two peaks, one peak is at fc/U=0.2 for sigma below 1.1; the other one is at fc/U=0.5 for sigma is higher than 1.1. This is similar to spectral data obtained with a NACA 0015 hydrofoil, but differs in the sense that the upper frequency peak is constant. The spectral characteristics of the NACA foil were such that there were two spectral branches with a bifurcation at $\sigma/2\alpha = 4$. the lower branch was at a constant value of fc/U = 0.2 whereas the upper branch dominated above $\sigma/2\alpha = 4$ where the frequency scaled with *cavity length, l,* fl/U.

3.3 Drag

Figure 3.5 is the plot of drag coefficient vs. sigma. The drag coefficient is defined as:

$$C_d = \frac{Drag}{1/2\,\rho U^2 ch}$$

Where:

C_d------Lift coefficient
Drag---Lift on the hydrofoil
?------- Density of water
U------ Velocity of upstream
c------- Cord length (0.081m)

h------- Height of the hydrofoil (0.19m)

Because of the hysteresis of drag measurement, the drag data are not very reliable. There is about a 20% relative error in the drag measurement.

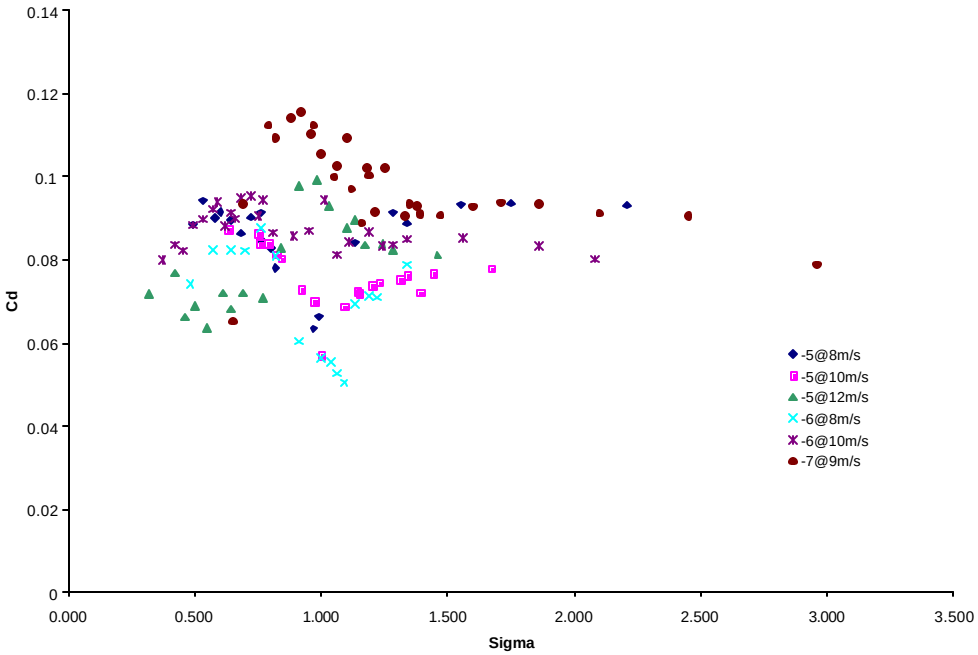

Figure 3.5 Drag coefficient

The drag spectrum for an angle of attack -5º is shown in Figure 3.6. Note that the drag spectrum has a pattern similar to the lift spectrum.

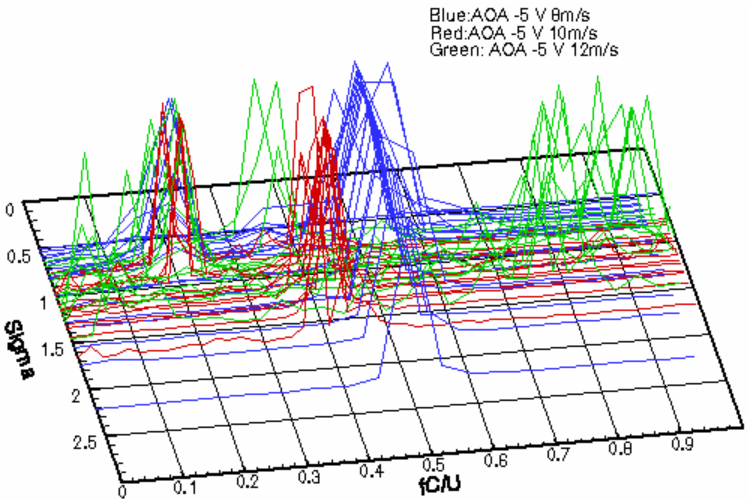

Figure 3.6 Drag spectra for angle of attack -5º

A more revealing plot is the ratio of lift to drag vs. sigma[2]. As shown in Figure 3.7, the L/D data show a similar trend to that for lift coefficient. Near sigma = 1.0, there is a peak of the ratio of lift to drag. Roughly speaking, about a 50% increase in L/D ratio is possible by stabilizing a cavity on the suction side of the foil.

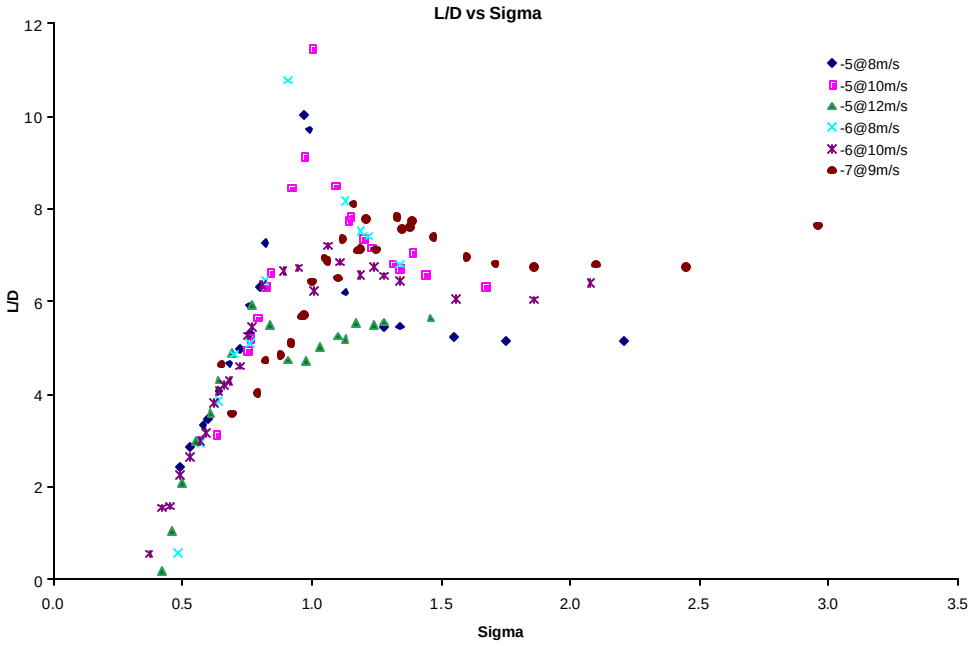

Figure 3.7 Ratio of lift to drag

3.4 Cavity Length Analysis

Although sometimes the cavity originated from mid-cord, only cavities observed to originate from the leading edge are considered in this analysis. As the cavitation process is highly dynamic, cavity length is herein defined as the maximum length. The measured cavity length at various angles of attack is presented in Figure 3.8 in the form l/c vs. $|\sigma/2\alpha|$. Also plotted are the partial and super-cavitation theory of Watanabe and the best-fit line to the data from the NACA 0015 foil. These data are similar to that observed for the NACA 0015 foil. In a consistent analysis the data should be correlated with $|\sigma/2(\alpha - \alpha_o)|$. However, as shown, the data collapse better if referencing to the zero lift angle is ignored. In looking at the design of the OK-2003 foil this observation may be logical from the viewpoint that the first half of the suction side is flat.

Note also that l/c exceeds 1 (supercavitation) at approximately $|\sigma/2\alpha| = 4$. This is he same result as for the NACA hydrofoil.

[2] Here the absolute value of lift is used to get the ratio of lift to drag.

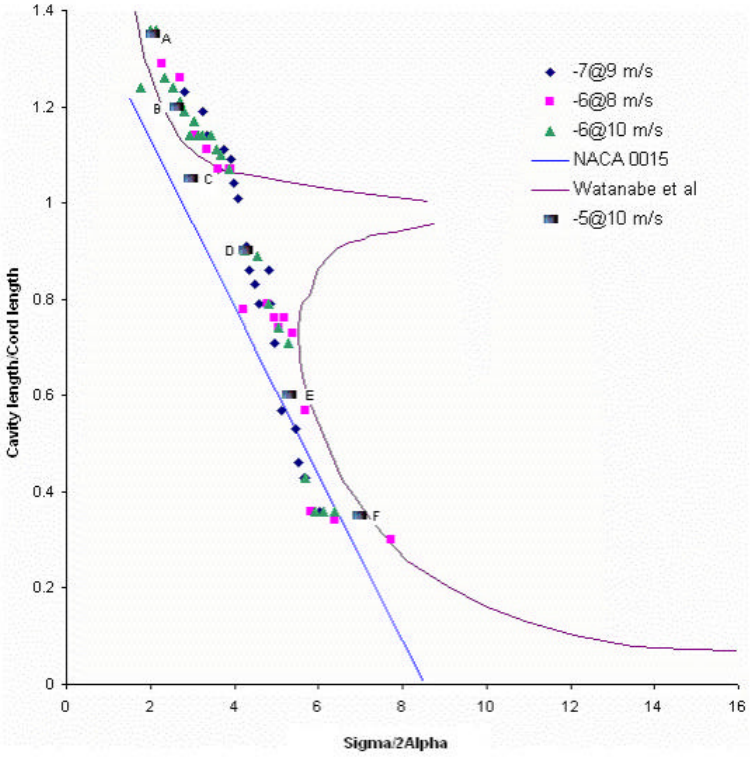

Figure 3.8 Cavity length

Photos corresponding to A - E in Figure 3.8 are presented in Figures 3.9 - 3.14.

4 CONCLUSIONS

The OK 2003 hydrofoil was tested over a range of angle of attack and cavitation number. Although some uncertainty exists in the drag data, preliminary analysis indicates that partial cavitation on the suction side of the blade leads to a significant increase in the lift to drag ratio. If the cavitation index is lowered below the optimal value, strong oscillations in lift occur. In Phase II of this study, it is proposed to consider methods for controlling these lift oscillations including the use of ventilation.

Cavity length data are similar to that observed on the NACA foil except that the data are displaced to higher values of $|\sigma/2(\alpha - \alpha_o)|$, suggesting that the suction side of the foil has a behavior similar to that for a flat plate, probably a result of the flat surface from the leading edge to mid-chord.

The preliminary results suggest that further study of this concept is warranted.

Ü Flow

Figure 3.9 -5@10m/s sigma=0.36 (A)

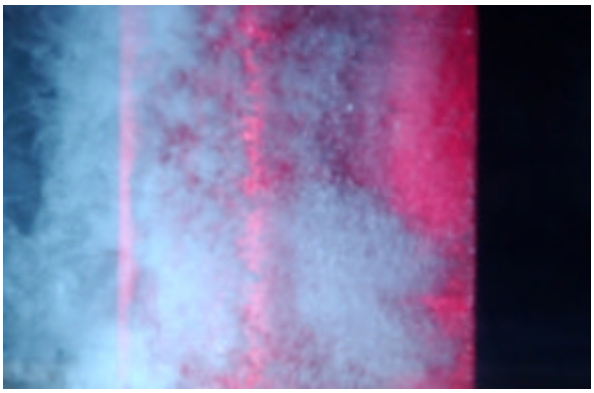

Figure 3.10 -5@10m/s sigma=0.46 (B)

Figure 3.11 -5@10m/s sigma=0.52 (C)

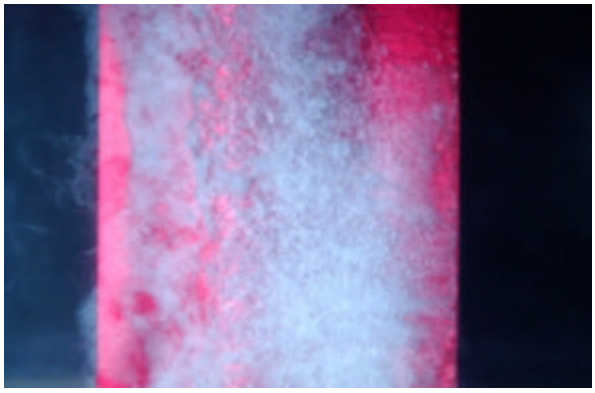

Figure 3.12 -5@10m/ssigma=0.75 (D)

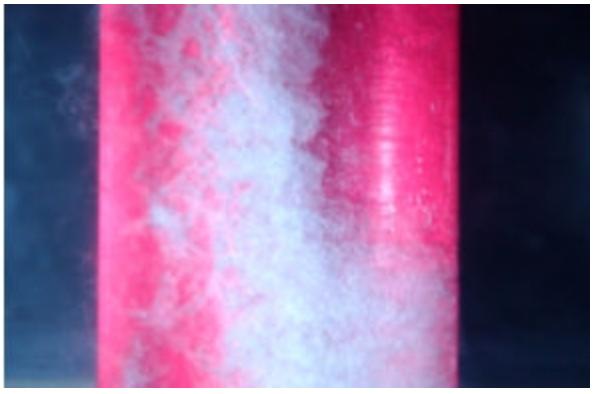

Figure 3.13 -5@10m/s sigma=0.93 (E)

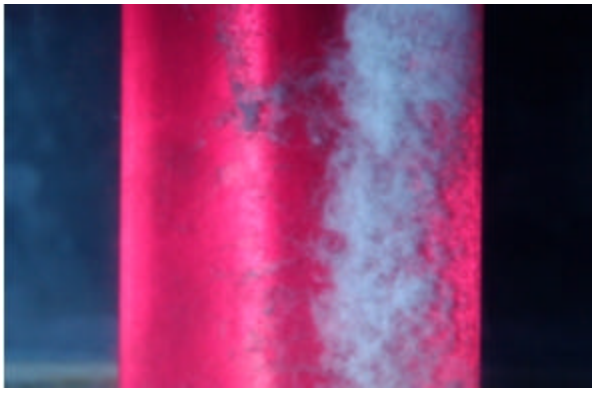

Figure 3.14 -5@10m/s sigma=1.22 (F)

5 References

Amromin, E., Hansberger, J., Wang, H and Martin Wosnik (2003) “Investigation Of A Low-Drag, Partially Cavitating Hydrofoil”, Fifth International Symposium on Cavitation (CAV2003) Osaka, Japan, November 1-4

6 Appendix: Dataset List

Table I dataset list

AOA	Velocity (m/s)	Comments
-3	various	for the angle of zero lift
-5	8	various cavitation number
-5	10	various cavitation number (w/photo)
-5	12	various cavitation number
-6	8	various cavitation number (w/video)
-6	10	various cavitation number (w/video)
-7	9	various cavitation number (w/video)

A full set of data has been forwarded to Mechmath in CD format.